Fluid Phase Equilibria 547 (2021) 113185

Contents lists available at ScienceDirect

Fluid Phase Equilibria

journal homepage: www.elsevier.com/locate/fluid

CO_2 absorption in amino acid-based ionic liquids: Experimental and theoretical studies

Narmin Noorani, Abbas Mehrdad*, Iraj Ahadzadeh

Department of Physical Chemistry, Faculty of Chemistry, University of Tabriz, Tabriz, Iran

ARTICLE INFO

Article history:
Received 21 February 2021
Revised 18 July 2021
Accepted 27 July 2021
Available online 30 July 2021

Keywords:
Amino acid-based ionic liquids
Thermodynamics
Absorption
DFT
CO_2

ABSTRACT

In this study, eight amino acid-based ionic liquids (AAILs) with 1-butyl-4-methyl pyridinium cation ([B_4MPyr][AA]s) were synthesized and characterized. The CO_2 absorption capacity of AAILs was studied using quartz crystal microbalance (QCM) at pressures up to 6 bars and at temperature 298.15 K. Based on the "deactivated model", the reaction equilibrium constant and Henry's law constant were calculated to evaluate the efficiency of AAILs for CO_2 absorption. The results indicate that CO_2 absorption capacities are in the order of [Arg] > [Lys] > [His] > [Tyr] > [Gly] > [Val] > [Ala] > [Pro]. The accessibility of more available amine groups in AAIL with arginate anion is the main factor for the high CO_2 absorption capacity. Also, the chemical absorption of CO_2 through carbamate formation was corroborated by spectroscopy of FT-IR. Beside, the density functional theory (DFT) method was also employed to confirm the adsorption energy of CO_2 onto AAILs with various anions.

1. Introduction

Global warming and the consequent adverse effects on the ecosystem represent one of the most major challenges of the 21st century. The carbon emission from fossil fuel combustion results in a consecutive increment of CO_2 concentration in the earth's atmosphere. Hence, consequent global warming and climate change have become the main challenge worldwide [1–3]. Carbon Capture and Storage (CCS) is an efficient method to mitigate carbon dioxide (CO_2) emissions into the atmosphere [4]. The CO_2 capture technologies are classified as solvent absorption (physical and chemical), adsorption (physical and chemical), membrane, and cryogenic separation [5,6]. The aqueous amine-based absorbents are known as one of the effective techniques for the chemical sorption of CO_2 in industries. However, the amine scrubbing process incurs high energy requisition for regeneration, solvent loss in regeneration, and amines corrosion [7]. Hence, novel materials or solvents such as ionic liquids (ILs) as good alternatives for efficacious capture of CO_2 have offered [8–13]. Recently, ionic liquids have been attracted as alternative CO_2 absorbents considerable attention due to their special characteristics such as strong solubility power, high polarity, high chemical and thermal stability, negligible volatility, and high affinity to acid gases [14–17]. Designing the physical and chemical properties of IL by selecting the favorable cations and anions, the CO_2 absorption capacities increase [18]. CO_2 absorption has been studied in amine-functionalized cation ILs over recent years [19–21]. Bates et al. [22] the high absorption capacity in amine-functionalized have been attributed to the chemical interactions. Khanna et al. [23] reported absorption capacity in amine-functionalized imidazolium cation ionic liquids threefold compared to non-functionalized ILs. Amino acid– based ionic liquids (AAILs) are amine-functionalized ILs that were introduced to increase the CO_2 absorption capacity of ILs [24,25]. AAILs show higher CO_2 absorption capacity than most pure amino acids, ethanolamine derivatives, and amino acid salts [26]. Recently, the CO_2 absorption in AAILs has been studied by some researchers [26–30]. Saravanamurgan et al. [31] have surveyed CO_2 absorption onto AAILs with ammonium cation and various anions containing lysine, histidine, asparagine, and glutamine. They have proposed that these ILs increments CO_2 absorption capacity via the chemisorptions process. Zhou et al. [32,33] have been studied amino–functionalized imidazolium and amino–functionalized tributyl phosphonium cation with some aminate anion. In a previous study, we have investigated the CO_2 absorption onto AAILs with imidazolium cation and different aminate (glycine, alanine, and valine) and glycinate anion has more CO_2 sorption capacity compared to alaninate and valinate [34]. Moreover, we have investigated CO_2 absorption onto some choline-aminate ionic liquids ([Cho][AA]s) with different aminate anions which indicates that maximum CO_2 absorption was related to glycinate anion [35]. To the best of our knowledge, no CO_2 absorption studies are unavailable in the literatures with pyridinium-cation and aminate-anion under applied conditions of the present study. In this study, CO_2 absorption in AAILs with

* Corresponding author.
E-mail address: a_mehrdad@tabrizu.ac.ir (A. Mehrdad).

https://doi.org/10.1016/j.fluid.2021.113185
0378-3812/

pyridinium cation and aminate anion was investigated. The eight AAILs: 1-butyl-4-methyl pyridinium glycinate ([B_4MPyr][Gly]), 1-butyl-4-methyl pyridinium alaninate ([B_4MPyr][L-Ala]), 1-butyl-4-methyl pyridinium valinate ([B_4MPyr][L-Val]), 1-butyl-4-methyl pyridinium prolinate ([B_4MPyr][L-Pro]), 1-butyl-4-methyl pyridinium tyrosinate ([B_4MPyr][L-Tyr]), 1-butyl-4-methyl pyridinium hisdinate ([B_4MPyr][L-His]), 1-butyl-4-methyl pyridinium lysinate ([B_4MPyr][L-Lys]), and 1-butyl-4-methyl pyridinium arginate ([B_4MPyr][L-Arg]) were synthesized by the neutralization technique. The synthesized amino acid-based ionic liquids characterized using proton nuclear magnetic resonance (^{1}HNMR). The CO_2 absorption in these [B_4MPyr][AA]s was measured using quartz crystal microbalance (QCM) at 298.15 K and pressures up to 6 bars. The absorption isotherms data were correlated using the "deactivated model" to calculate the thermodynamic parameters. The corresponding adsorption parameters, reaction equilibrium constant and Henry's law constant were calculated to evaluate the CO_2 absorption performance in [B_4MPyr][AA]s. The chemical adsorption of CO_2 due to the formation of carbamic acid has been corroborated by spectroscopy of FT-IR. The efficacy of the ionic liquid anion on the CO_2 absorption capacity has been investigated. Moreover, DFT calculated was applied to survey the interactions among the CO_2 and [B_4MPyr][AA]s. Also, NBO analysis was applied for exploring the bond specifics and donor-acceptor interactions.

2. Experimental section

2.1. Materials

4–Methylpyridine (purity > 0.99), 1–Bromobutane (purity > 0.99), Toluene (purity > 0.99), Ethanol (purity ≥ 0.999), and Ethyl acetate (purity > 0.99) were purchased from Merck. Glycine (Gly), L-Alanine (Ala), L-Valine (Val), L–Proline (Pro), L–Histidine (His), L-Lysine (Lys), L–Tyrosine (Tyr), and L–Arginine (Arg) were Sigma Aldrich products (purity ≥ 0.99). The properties of amino acids and their structural are shown in Table 1 The gas of CO_2 (purity > 0.9999 is mass fraction) was applied in gas absorption tests.

2.2. Synthesis of ionic liquid

2.2.1. 1–Butyl–4–methylpyridinium bromide

Direct alkylation of 4–methyl pyridine with 1-bromobutane in toluene as solvent at $T = 323$ K under argon atmosphere was used to synthesis 1–butyl–4–methyl pyridinium bromide ([B_4MPyr][Br]) [36,37]. The purification procedure is the same as described previously [38]. The water amount of the ionic liquid measured using a Karl-Fischer titrator (720-KSS-Metrohm Herisau, Switzerland). The synthesized ionic liquid was characterized using ^{1}HNMR (Bruker Av-400, Germany) and FT-IR (Bruker, Tensor 27, Germany) spectroscopy. The purity of the synthesized ionic liquid was obtained by the procedure expressed in the literature [39]. ^{1}HNMR and FT-IR spectra of synthesized [B_4MPyr][Br] are shown in Figs. S1 and S2 (Supporting Information). The purity of [B_4MPyr][Br] was obtained > 0.98.

2.2.2. 1–Butyl–4– methylpyridinium based amino acid

1–Butyl–4–methyl pyridinium based amino acid ionic liquids, [B_4MPyr][Gly], [B_4MPyr][L-Ala], [B_4MPyr][L-Val], [B_4MPyr][L-Pro], [B_4MPyr][L-His], [B_4MPyr][L-Arg], [B_4MPyr][L-Tyr] and [B_4MPyr][L-Lys] were synthesized as expressed in the previous literature [34]. In this study, for easier reading, [B_4MPyr][AA]s were named as IL1, IL2...etc. in Table 2. Briefly, 1–butyl–4–methyl pyridinium hydroxide ([B_4MPyr][OH]) was obtained through anion exchange resin of aqueous solution of [B_4MPyr][Br]. The exchange of bromide anion with hydroxide was performed in the glass column contains ion exchange resin. Prepared pyridinium hydroxide ([B_4MPyr][OH]) aqueous solution was added dropwise to excess equimolar aqueous Glycine, L-Alanine, L-Valine, L–Proline, L–Histidine, L-Lysine, L–Tyrosine, or L–Arginine (1.2 equivalent) solutions, and stirred at ambient temperature for 48 h. Then water amount was removed by a rotary evaporator for at least 8 h at 352 K. The unreacted amino acids were eliminated via precipitation in absolute ethanol. The synthesis [B_4MPyr][AA]s evaporated to remove ethanol under a vacuum for 4 h at 338 K. The water quantity of the [B_4MPyr][AA]s was determined about 0.01 mass fraction using a Karl–Fischer titrator. The [B_4MPyr][AA]s purity (>98%) was characterized using the ^{1}HNMR in D_2O. ^{1}H NMR spectra of [B_4MPyr][AA]s are shown in Figs. S3–S10 (Supporting Information). Also the ^{1}H NMR spectrum of the L-arginine which used for the synthesis is shown in Fig. S11 (Supporting Information).

2.3. Characterization of aminate anion [B_4MPy][AA]s

FT-IR spectrometer was used to recording the FT-IR spectra of [B_4MPyr][AA]s before and after CO_2 absorption in the wavenumber range of 400–4000 cm^{-1}.

2.4. Gas adsorption apparatus

QCM sensor was used to evaluate gas absorption. The adsorption cell includes an 8 MHz AT-cut quartz crystal utilized in the electrical oscillator circuit. QCM is based on the mass effect on the observed frequency of a piezoelectric AT-cut quartz crystal. AT- cut quartz crystal of 8 MHz resonant frequency was used in the electrical oscillator circuit, in the absorption cell. The oscillator was applied using a stabilized potential of 5.0 V and the quartz crystal frequencies was evaluated by a 10 digits frequency counter (MASTECH Multi-function Counter MS6100). The Quartz Crystal Microbalance composed of a light crystal of piezoelectric quartz sandwiched among two golden electrodes that produce an alternating electric field across the crystal, causing the vibrational movement of the crystal at its resonant frequency. The frequency is a function of the crystal mass and variation of frequency,ΔF, is arising from a mass variation, Δm, as follows:

$$\Delta F = -k\Delta m \tag{1}$$

where k is a proportionality constant that contains geometrical and physical properties of the crystal [40–42]. The absorption capacity of adsorbent in terms of mole fraction (x_{CO_2}) has been evaluated by the following equation:

$$x_{CO_2} = \frac{\frac{\Delta F_S}{M_{CO_2}}}{\frac{\Delta F_S}{M_{CO_2}} + \frac{\Delta F_C}{M_{[B_4MPyr][AA]}}} \tag{2}$$

where ΔF_C is the difference frequencies between the coated (quartz crystals which coated with a thin layer of the ILs) and the uncoated crystal (empty quartz crystals). ΔF_S is the difference frequencies of the coated crystal in a vacuum and coated crystal after the gas adsorption.

2.5. Chemical absorption thermodynamic model

The absorption mechanism of CO_2 in [B_4MPyr][AA]s has two distinguished physical and chemical absorption contributions. The "deactivated model" was utilized to describe the chemical and physical absorption of CO_2 in amino acid-based ionic liquids (AAILs) [43–45]. The physically absorption and chemically absorption of CO_2 are represented as follows:

$$CO_{2(g)} \leftrightarrow CO_{2(l)} \tag{3}$$

$$IL_{(l)} + CO_{2(l)} \overset{K_x}{\longleftrightarrow} IL_{(l)} - CO_2 \tag{4}$$

Table 1
Properties and molecular structures of amino acids [60].

Amino acid	Abbreviation	Molecule weight	pK_a (α-NH_3^+)	Molecular structure
Glycine	Gly	75.07	9.60	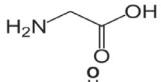
L–Alanine	Ala	89.09	9.87	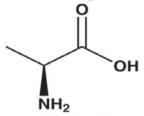
L–Valine	Val	117.15	9.62	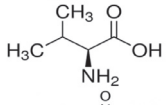
L–Proline	Pro	115.13	10.60	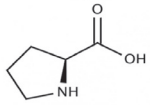
L–Tyrosine	Tyr	181.19	9.11	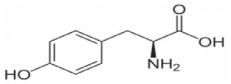
L–Histidine	His	155.15	9.17	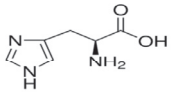
L–Lysine	Lys	146.19	8.95	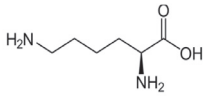
L–Arginine	Arg	174.20	9.04	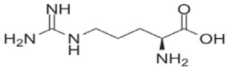

Table 2
Abbreviation of amino acid-based ionic liquids.

$[B_4MPyr][AA]s$	Abbreviation
$[B_4MPyr][L\text{-}Arg]$	IL1
$[B_4MPyr][L\text{-}Lys]$	IL2
$[B_4MPyr][L\text{-}His]$	IL3
$[B_4MPyr][L\text{-}Tyr]$	IL4
$[B_4MPyr][Gly]$	IL5
$[B_4MPyr][L\text{-}Ala]$	IL6
$[B_4MPyr][L\text{-}Val]$	IL7
$[B_4MPyr][L\text{-}Pro]$	IL8

The value of physically absorption CO_2 ($x_{CO_{2(l)}}$) in the ILs corresponding to CO_2 pressure (P_{CO_2}) and describe by Henry's law by the following equation:

$$P_{CO_2} = Hx_{CO_{2(l)}} \tag{5}$$

where H is Henry constant. The adsorbed CO_2 undergoes a reaction after physically sorption; hence the amount of chemically sorption CO_2 in the IL can be expressed using the equilibrium constant:

$$K_x = \frac{x_{CO_2-\mathrm{IL}_{(l)}}}{x_{\mathrm{IL}_{(l)}} x_{CO_{2(l)}}} \tag{6}$$

In the IL solution, the total mole fractions of CO_2 is the sum of physically absorbed CO_2 and the chemically reacted as IL–CO_2 complex.

$$x_{CO_2} = x_{CO_{2(l)}} + x_{CO_2-IL_{(l)}} \tag{7}$$

On the based deactivated model, the total mole of IL is the sum of the moles of IL–CO_2 complex, IL, and the deactivated IL. The mole of deactivated IL indicates the mole of IL that does not react with CO_2 due to self–association. The mole fraction of IL can be reported by the following equation:

$$x_{IL_{(l)}} = 1 - x_{CO_{2(l)}} - x_{CO_2-IL_{(l)}} - x_{deactivated-IL_{(l)}} \tag{8}$$

Rearranging Eqs. (4)–(6), the total mole fractions of CO_2 in the IL as follows:

$$x_{CO_2} = \frac{p_{CO_2}}{H} + \frac{K_x p_{CO_2}(C - \frac{p_{CO_2}}{H})}{H + K_x p_{CO_2}} \tag{9}$$

where $C = 1 - x_{deactivated-IL_{(l)}}$ is experimental constant.

2.6. Computational methods

To evaluate the carbon dioxide absorption mechanism, DFT calculations were performed for $[B_4MPyr][AA]$ (IL1, IL2, IL3, IL4, IL5, IL6, IL7, and IL8) with the Gaussian 03 program [46]. In order to, based on the partial charge distribution several structures were considered for $[B_4MPyr][AA]$. The full optimization of structures was performed using the B3LYP–D3/6–311 G* (d, p) level of theory [47,48]. The most stable configurations were suggested to study

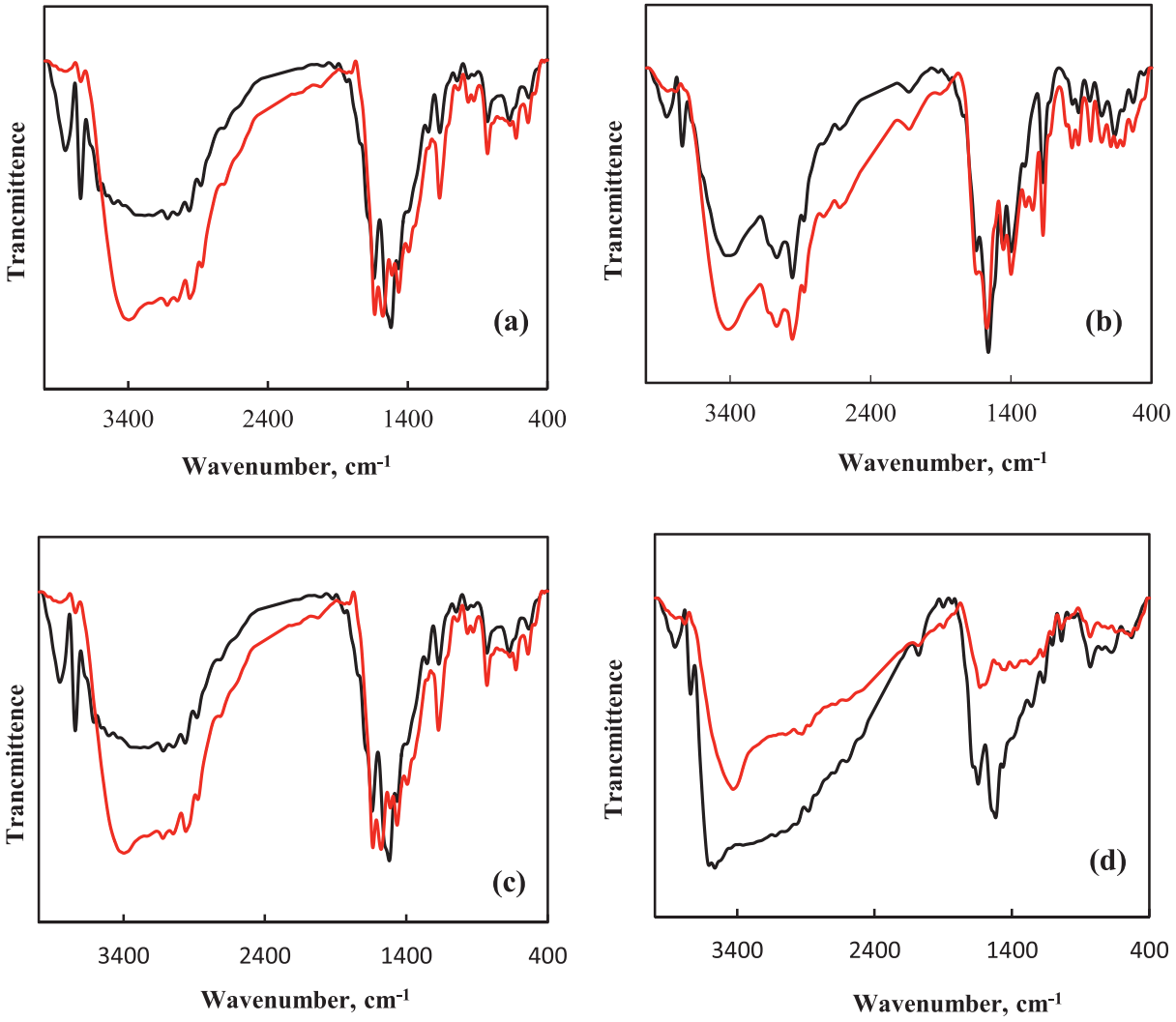

Fig. 1. FT–IR of (a) IL1; (b) IL2; (c) IL3; (d) IL4; (e) IL5; (f) IL6; (g) IL7; (h) IL8 before and after CO_2 absorption (–red: IL–CO_2; black: IL) (For interpretation of the references to color in this figure legend, the reader is referred to the web version of this article.).

CO_2 absorption. The absorption energy (E_{ads}) is obtained using the following equation [49–51]:

$$E_{ads} = E_{tot}(IL - CO_2) - E_{tot}(IL) - E_{tot}(CO_2) \quad (10)$$

The electronic specifics such as charge transfer analysis, natural bond orbital (NBO) analysis, energy of highest occupied molecular orbital (HOMO), and the energy of lowest unoccupied molecular orbital (LUMO) were utilized by the NBO 3.1 program [52] included in the Gaussian 03 program at the B3LYP–D3/6–311 G*(d, p) level of theory.

3. Result and discussion

3.1. Characterization of aminate [B_4MPyr][AA]s after CO_2 absorption

^{13}C NMR and FT-IR spectroscopy were applied to evaluate the suggested reaction pathway of [B_4MPyr][AA] with CO_2. The characteristic FT–IR peak corresponding to C=O of –COO at 1420, 1650 cm^{-1} and the peak corresponding to N–H stretch of $–NH_2$ at 3400–3000 cm^{-1} are observed for all the aminate [B_4MPyr][AA] synthesized [51]. FT–IR spectra of the IL1, IL2, IL3, IL4, IL5, IL6, IL7, and IL8 after and before CO_2 absorption are illustrated in Fig. 1. The reaction between CO_2 and aminate anion of ionic liquids produced carbamic acid. FT–IR spectra of [B_4MPyr][AA] after CO_2 absorption indicates a band related to the O–H stretch of carbamic acid in the range 2700–3000 cm^{-1}. Analyze of FT–IR peaks in Fig. 2 (a) IL1–CO_2: [Arg] contains two secondary and two primary amine groups. The peak belongs carbonyl of carbamate has been observed in around 1510–1630 cm^{-1}. (b) IL2–CO_2: [Lys] has two primary amine groups and the reaction of these groups with CO_2 leads to secondary amine (–NH) and forming a carbamic acid. Therefore in IL2–CO_2 a peak observed around 1570 cm^{-1} corresponding to the carbonyl of carbamate. (c) Analysis of FT–IR peaks IL3–CO_2 manifest that the characteristic peak related to carbamic acid at 2700 cm^{-1}. The bands related to the carbonyl of carbamate are observed in the region 1520–1650 cm^{-1}. The molecular structure of [His] indicates that it has one $–NH_2$ group and one –NH group. Hence, CO_2 can react with both the groups of primary amine ($–NH_2$) and secondary amine (–NH). The reaction of CO_2 with the primary amine $–NH_2$ will lead to secondary amine (–NH) and forming a carbamic acid. The C=O peak in carbamate overlaps with the COO^- in aminate. (d) IL4–CO_2: [Tyr] contains one $–NH_2$ group and reacted with CO_2 to produce carbamic acid; therefore a peak in the range 2550–3000 cm^{-1} attributed to the stretch of O–H in carbamic acid. (e) IL5–CO_2, (f) IL6–CO_2, and (g) IL7–CO_2 reveals that the signals at 1420 and 1590 cm^{-1} are related to asymmetric stretch and symmetric stretch of carbonyl in COO^-. The signal at 1180 cm^{-1} after CO_2 absorption corresponding to N–C in carbamate. (h) IL8–

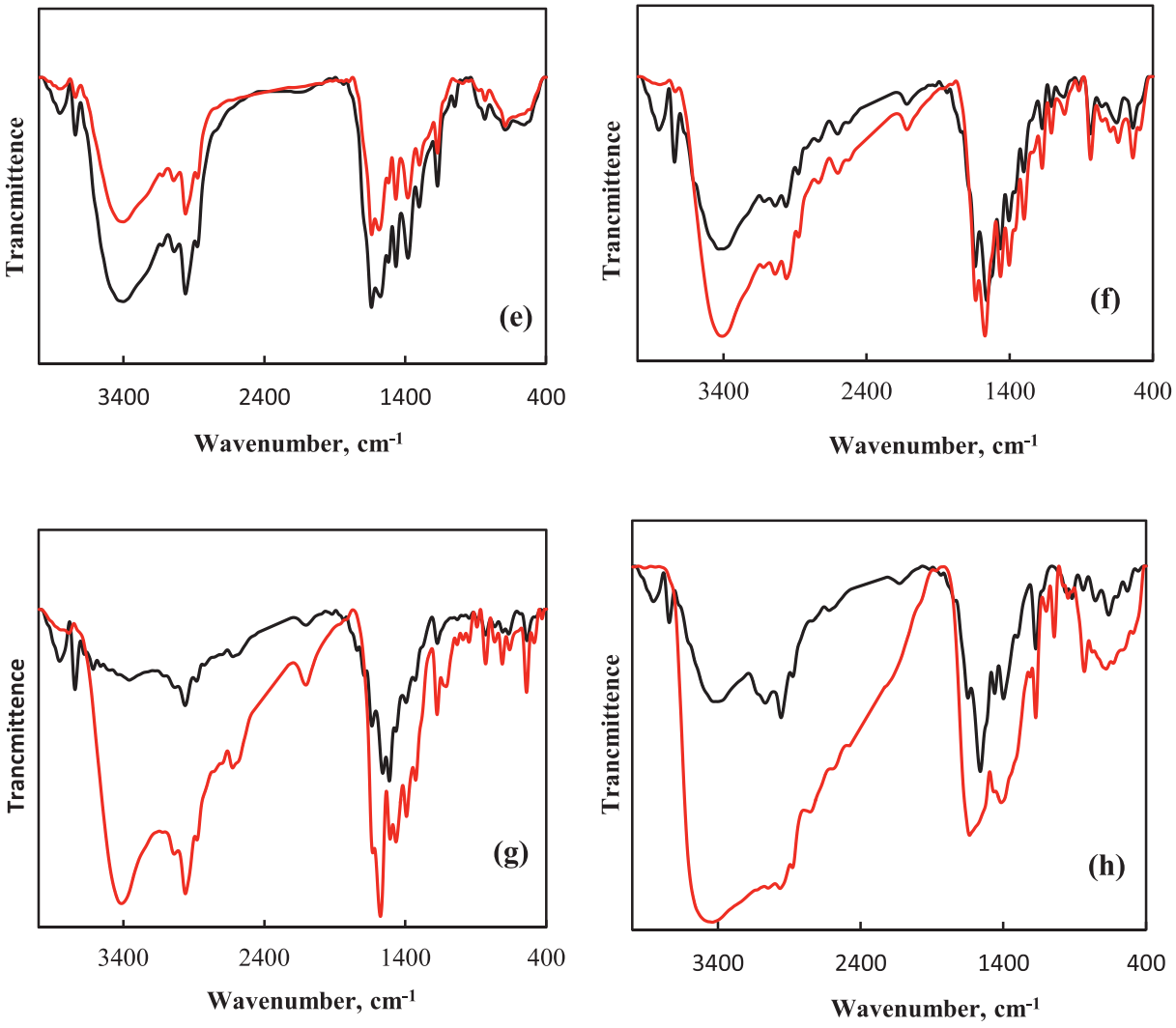

Fig. 1. Continued

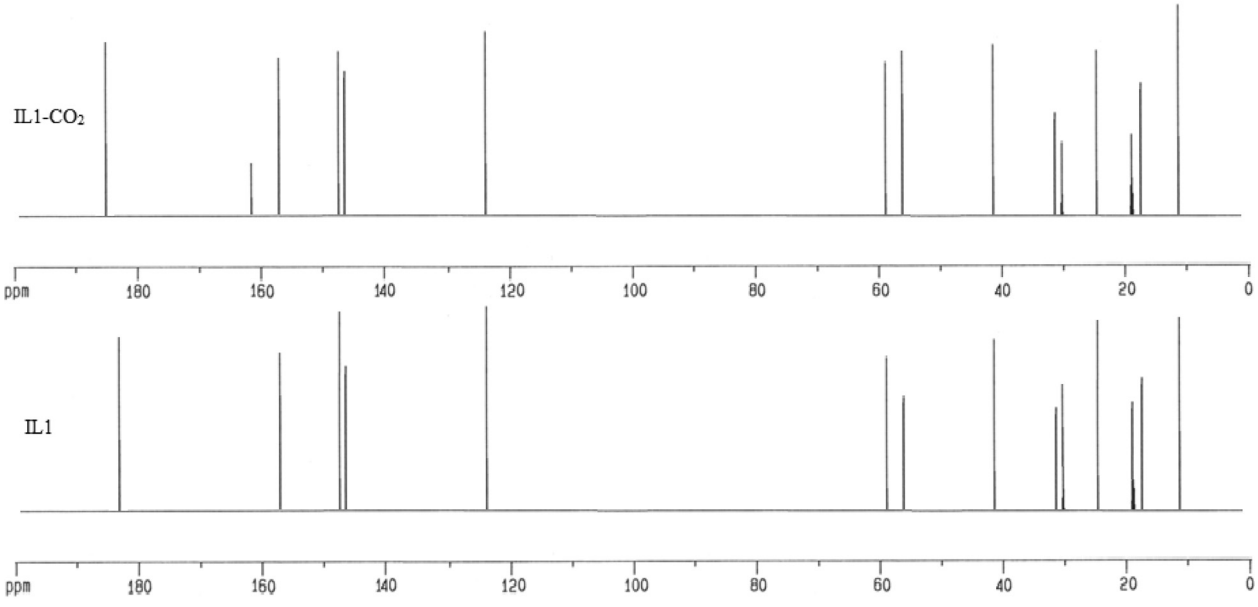

Fig. 2. ^{13}C NMR spectra of IL1 before and after CO_2 absorption.

Table 3
CO_2 absorption capacity in terms mole fraction (x_{CO_2}) of [B_4MPyr][AA]s at pressures (p) up to 6 bars and temperature T = 298.15 K.

T = 298.15K		T = 298.15 K		T = 298.15 K		T = 298.15 K	
P /bar	x_{CO_2}	P /bar	x_{CO_2}	P /bar	x_{CO_2}	P /bar	x_{CO_2}
IL1		IL2		IL3		IL4	
0.164	0.097	0.346	0.097	0.223	0.062	0.185	0.056
0.357	0.189	0.632	0.167	0.491	0.127	0.486	0.132
0.654	0.276	0.880	0.215	0.699	0.174	0.697	0.174
0.945	0.342	1.068	0.243	0.856	0.203	1.029	0.230
1.500	0.420	1.500	0.309	1.009	0.226	1.500	0.290
2.000	0.471	2.000	0.366	1.500	0.296	2.000	0.325
2.500	0.504	2.500	0.402	2.000	0.341	2.500	0.364
3.000	0.531	3.000	0.444	2.500	0.388	3.000	0.387
3.500	0.554	3.500	0.468	3.000	0.415	3.500	0.412
4.000	0.568	4.000	0.488	3.500	0.446	4.000	0.433
4.500	0.583	4.500	0.507	4.000	0.466	4.500	0.453
5.000	0.594	5.000	0.524	4.500	0.482	5.000	0.463
5.500	0.605	5.500	0.542	5.000	0.499	5.500	0.476
6.000	0.613	6.000	0.554	5.500	0.513	6.000	0.487
				6.000	0.524		
IL5		IL6		IL7		IL8	
0.226	0.070	0.234	0.074	0.239	0.066	0.245	0.080
0.497	0.141	0.375	0.128	0.389	0.104	0.502	0.130
0.674	0.167	0.590	0.172	0.618	0.144	0.713	0.168
1.008	0.222	0.777	0.212	0.764	0.165	0.987	0.197
1.500	0.283	1.022	0.248	0.996	0.197	1.500	0.246
2.000	0.327	1.500	0.303	1.500	0.251	2.000	0.279
2.500	0.362	2.000	0.342	2.000	0.288	2.500	0.310
3.000	0.391	2.500	0.375	2.500	0.318	3.000	0.326
3.500	0.411	3.000	0.401	3.000	0.342	3.500	0.338
4.000	0.427	3.500	0.416	3.500	0.361	4.000	0.351
4.500	0.440	4.000	0.433	4.000	0.373	4.500	0.360
5.000	0.453	4.500	0.445	4.500	0.389	5.000	0.368
5.500	0.466	5.000	0.454	5.000	0.398	5.500	0.374
6.000	0.475	5.500	0.465	5.500	0.409	6.000	0.379
		6.000	0.469	6.000	0.414		

Standard uncertainties are $u_r(x_{CO_2}) = 1\%$, $u(T) = 0.05$ K, and $u_r(p) = 1\%$.

CO_2: [Pro] has one secondary amine group. The peak in the region 3000–3400 cm^{-1} is attributed to the N–H and the signal in the range 2530–3000 cm^{-1} corresponding to the O–H stretch of carbamic acid. ^{13}C NMR spectra also can be confirm the formation of aminate group [52]. ^{13}C NMR spectra of IL1 before and after CO_2 absorption are presented in Fig. 2. A peak at δ= 163 ppm confirmed the presence of aminate group due to interaction of anion of IL with CO_2.

3.2. Effect of pressure on CO_2 absorption

The CO_2 absorption capacity data in eight different amino acid-based ionic liquids contain IL1, IL2, IL3, IL4, IL5, IL6, IL7, and IL8 were measured at temperature of 298.15 K. The obtained experimental absorption capacities are given in Table 3. CO_2 absorption capacity in IL1, IL2, IL3, IL4, IL5, IL6, IL7, and IL8 are 0.613 mol/mol, 0.554 mol/mol, 0.524 mol/mol, 0.487 mol/mol, 0.475 mol/mol, 0.469 mol/mol, 0.414 mol/mol, and 0.379 mol/mol, respectively at 6 bar and 298.15 K. The CO_2 absorption capacity in these ionic liquids were compared to the value obtained for CO_2 absorption in other ionic liquids under the same condition in Table 4. The relationship between absorption capacity and pressure is illustrated in Fig. 3. These isotherms show that the absorption capacity increments with incrementing pressure, which shows a similar pattern as most of acid gases [53,54]. As seen in Fig. 3, the CO_2 absorption isotherms in [B_4MPyr][AA]s have a non-linear behavior. CO_2 absorption capacity increments dramatically in the low-pressure region, while it rises slightly and almost linearly in the high-pressure region. This phenomenon represents that CO_2 is chemically absorbed by [B_4MPyr][AA]s. A similar results were reported for amino acid-based ILs, tri-

Table 4
Comparison of CO_2 absorption capacity in aminate anion at Temperature 298.15 K.

AAILs	P / bar	Mol CO_2 /mol AAIL	Ref.
IL1	2	0.47	This work
IL2	2	0.37	This work
IL3	2	0.34	This work
IL4	2	0.32	This work
IL5	2	0.33	This work
IL6	2	0.34	This work
IL7	2	0.29	This work
IL8	2	0.28	This work
[bmim][Arg]	2	0.62	[23]
[bmim][Lys]	2	0.48	[23]
[bmim][His]	2	0.45	[23]
[bmim][Pro]	2	0.32	[23]
[VBTMA][Arg]	1	0.83	[55]
[VBTMA][Lys]	1	0.66	[55]
[VBTMA][Hist]	1	0.46	[55]
[VBTMA][Gly]	1	0.47	[55]
[VBTMA][Ala]	1	0.29	[55]
[VBTMA][Pro]	1	0.38	[55]
[VBTMA][Arg]	0.7	0.45	[56]
[VBTMA][Pro]	0.7	0.27	[56]

hexyl(tetradecyl)phosphonium glycinate ([P14666][Gly]), isoleucinate ([P14666][Ile]), 2-cyanopyrrolide ([P14666][2-CNpyr]), 3-(trifluoromethyl)([P14666][3-CF3pyra]), prolinate ([P14666][Pro]), and methionate ([P14666][Met]), which were experimentally shown to react with CO_2 in a 1:1 stoichiometry [55–57]. Also, they have shown that the isotherms can be subdivided into two distinct parts: a sharp increase at low pressures due to chemical absorption and a marginal increase in capacity at higher pressures which is typical for physical absorption [58,59]. Nonetheless, it was shown that the vast majority of the uptake was due to chemical absorption which this results is in good agreement with our results reported.

3.3. Effect of anion on CO_2 absorption

To study the effect of anion, the CO2 absorption capacity of [B_4MPyr] with various anions were investigated at pressures up to 6 bars and temperature 298.15 K. The comparisons of CO_2 absorption capacity in IL1, IL2, IL3, IL4, IL5, IL6, IL7, and IL8 in Fig. 3 show that among the aminates investigated, [Arg], [Lys], and [His] due to basic nature and polar side chains have the high CO_2 absorption capacity in contrast to that with the other [B_4MPyr][AA]s. This behavior may be due to strong acid-base interactions in these ionic liquids in comparison with the other [B_4MPyr][AA]s. [Arg] and [Lys] have higher CO2 absorption with 0.613 and 0.554 mol/mol, respectively, followed by [His], [Tyr], [Gly], [Ala], [Val], and [Pro]. The [Arg] anion comprises two primary amines and two secondary amines; therefore, a higher chance for CO_2 is available to react with one or more of these four accessible amine sites. [Lys] has the CO_2 absorption capacity lower than [Arg] and this behavior may be attributed to two primary amine groups in [Lys]. [His] contains a pentagonal ring with one secondary and one primary amine group, has less capacity for CO_2 with 0.524 mol/mol. [Hist] due to steric hindrance and low efficacies of the secondary amine group [His] allocates third place after [Arg] and [Lys] (Fig. 3). The amine group number and alkyl chain length of cation are two main factors that affect the process of CO_2 absorption. The results indicate that the effect of the amine group's number is more important than the alkyl chain length in the CO_2 absorption process. The remainder of the anions ([Gly], [Ala], [Val]) has one primary amine group and a nonpolar aliphatic side chain. All these anions display less or more similar capacities of CO_2 absorption, [Gly], [Ala], [Val], and [Pro] have 0.475 mol/mol, 0.469 mol/mol, 0.414 mol/mol,

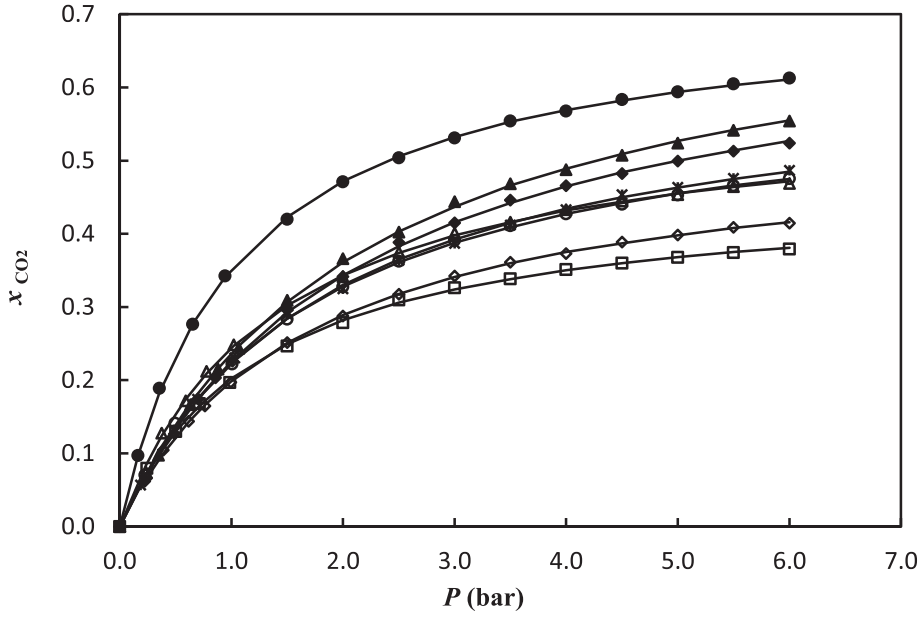

Fig. 3. The CO_2 solubility in (●) IL1; (▲) IL2; (♦)IL3; (*) IL4; (○) IL5; (Δ) IL6; (◇) IL7; (□) IL8 at temperatures of 298.15 K; (–) Fitted to Eq. (9).

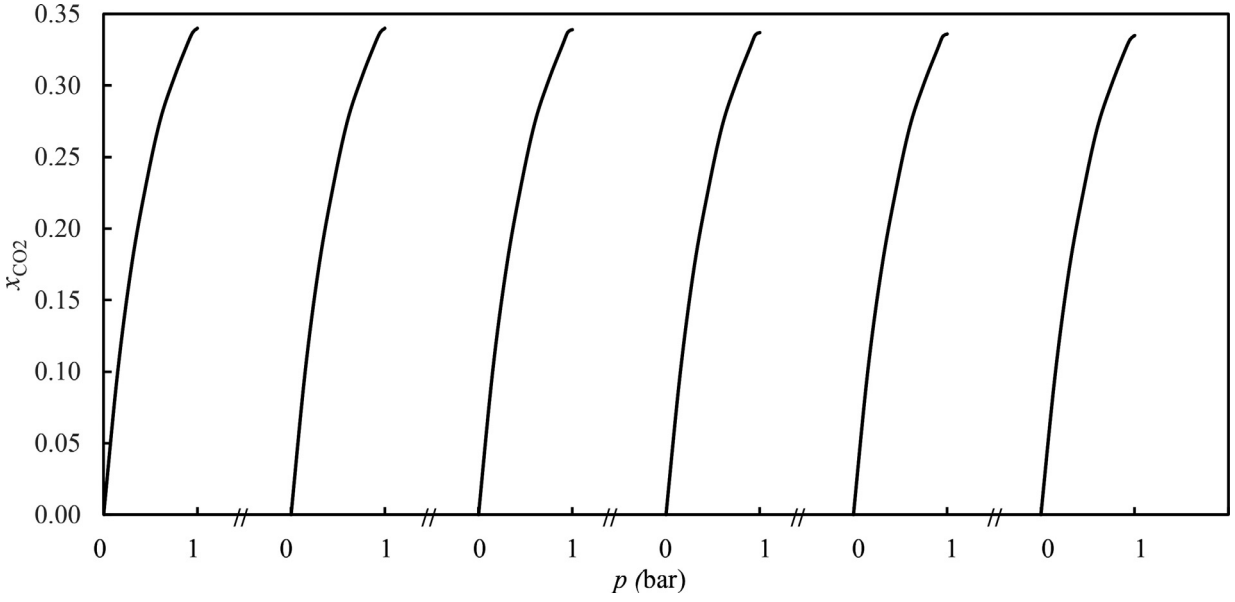

Fig. 4. The CO_2 absorption capacity of IL1 at $T = 298.15$ K in six absorption/desorption cycles.

and 0.379 mol/mol, respectively, as illustrated in Fig. 3. The differences in the absorption capacities can be due to the variations in their physical and chemical properties of amino acids. [Gly], [Ala], and [Val] have similar amine groups, but the CO_2 absorption by [Ala] anion is less than [Gly] anion. This phenomenon is attributed to a longer alkyl chain length of the [Val] anion, which increases its steric hindrance versus the CO_2 absorption. Also, the ionic liquid with [Pro] anion indicates minimum CO_2 absorption capacity. This behavior can be attributed to the molecular structure of [Pro] (Table 1). Based on Table 1, the amine group in this aminate is available in a pentagonal ring and behaves as a secondary amine. Hence, the availability of 'N' atom in [Pro] anion to react with CO_2 is lower due to steric hindrances, eventuating is lesser the CO_2 absorption capacity. These results are similar to those reported in the literature that AAILs with more than one amine site have shown higher CO_2 absorption capacity than the AAILs with only one primary amine group. Sistla and Khanna [23] have been investigated various AAILs and observed that CO_2 absorption capacities were as order: [bmim][Arg] (0.62 mol CO_2/mol IL)> [bmim][Lys] (0.48 mol CO_2/mol IL) > [bmim][His] (0.45 mol CO_2/mol IL) > [bmim][Pro] (0.32 mol CO_2/mol IL) at 298 K & 2 bar. Santiago et al. [61] have been reported that [bmim][Met] and [bmim][Gly] present similar and the highest CO_2 sorption capacity (0.035 g CO_2/g IL), while [bmim][Pro] shows lower one (0.020 g CO_2/g IL). Saravanamurugan et al. [31] show that ammonium-based, $[N_{66614}]$[Arg] is CO_2 sorption at 1.0 molCO_2/mol IL. Raja Shahrom et al. [62] have been reported CO_2 absorption in forms of AAILs for eight anions [Gly], [Ala], [Ser], [Tau], [Arg], [Lys], [Hist], and [Pro] with ammonium based, [VBTMA], cation. They indicate that [VBTMA][Arg] gave the highest capacity of CO_2 absorption with 0.83 mol/mol and [VBTMA][Ala] has the least capacity of CO_2 absorption with 0.29 mol/mol. In another study, they investigated the CO_2 sorption

Table 5
Henry's law constant (H), reaction equilibrium constant (K_x), experimental constant (C), the correlation coefficient (R^2) and absolute average relative deviation ($AARD$) for CO_2 absorption in [B_4MPyr][AA]s at temperature $T = 298.15$ K.

[B_4MPyr][AA]s	H (bar)	K_x	C	R^2	$AARD\%$
IL1	121.88	117.03	0.70	0.9998	0.52
IL2	116.77	52.75	0.74	0.9996	0.74
IL3	111.65	51.22	0.69	0.9997	0.73
IL4	90.22	48.81	0.61	0.9995	0.74
IL5	85.29	48.97	0.59	0.9995	0.76
IL6	66.03	47.87	0.56	0.9994	0.64
IL7	76.21	45.44	0.51	0.9998	0.65
IL8	57.98	45.40	0.44	0.9993	0.74

$AARD\% = \frac{100}{n}\sum\left|\frac{x_{CO_2}^{cal} - x_{CO_2}^{exp}}{x_{CO_2}^{exp}}\right|$

of the monomer, amino acids ionic liquids (AAILs) and the polymer, amino acid-based polymerized ionic liquids (AAPILs) at 1 bar, 298 K. They reported poly[VBTMA][Arg] gave higher CO_2 sorption at 0.530 mol fraction compared to poly[VBTMA][Pro] at 0.380 mol fraction. Also, monomer of [VBTMA][Arg] gave higher CO_2 sorption at 0.454 mol fraction compared to [VBTMA][Pro] at 0.274 mol fraction in low pressure (P_{eq} 0.7 bar) at 298 K [63].

3.4. Parameters of thermodynamic model

In the CO_2 absorption process, the values of Henry's law constant (H) and the reaction equilibrium constants ($K_{x)}$ are related to the CO_2 absorption capacity. So, these parameters can be obtained by fitting the experimental absorption data and then evaluate the absorbent for the CO_2 absorption process. The "deactivated model" clearly demonstrated that CO_2 can be absorbed both chemically and physically in [B_4MPyr][AA]s. The physical absorption is related to Henry's law constant (H), and the reaction equilibrium constant (K_x) is related to the chemical absorption. To achieve a deep understanding of the CO_2 absorption phenomenon in [B_4MPyr][AA]s, it is necessary to assess the contributions of chemical and physical individually. For this purpose, the non-linear regression was used to correlating experimental absorption data to Eq. (8). The correlation of experimental absorption data reveals that the CO_2 absorption in [B_4MPyr][AA]s is excellently correlated by Eq. (8) and CO_2 is absorbed both chemically and physically in [B_4MPyr][AA]s. The obtained parameters H and K_x along with the correlation coefficient R^2 were tabulated in Table 5. The results manifest that the correlation coefficients R^2 higher than 0.999 which implies to the applicably of the suggested model. Also, the values of H and K_x increase in the order of [Arg] > [Lys] > [His] > [Tyr] > [Gly] > [Val] > [Ala] > [Pro]. In Eq. (8) the primary term and second term indicate physical absorption and chemical absorption, respectively. The high quantities of the chemical reaction constant (K_x) reveals that chemical absorption has high contribution in the CO_2 absorption process while the higher values of Henry constant (H) reveals that physical absorption has low contribution in the CO_2 absorption process in [B_4MPyr][AA]. Therefore, the high values of K_x represent a strong driving force in the formation complex of the [B_4MPyr][AA]s with CO_2.

3.5. Regeneration efficiency of IL1

Regeneration is one of the important factors in investigating the absorption efficiency. In order to measure the reuse capacity, six cycles of CO_2 absorption/desorption experiment on the IL1 are plotted in Fig. 4. For regeneration experiment, CO_2 absorption is tested at 1 bar and 298.15 K and desorption under vacuum at temperature of 298.15 K and 90 min to omit CO_2. The absorption/desorption amount represents that CO_2 was perfectly omitted in 90 min and the absorption amount is stable in six cycles. The reduction in CO_2 absorption capacity of the regenerated IL1 was apperceived to be about 1 % in the six cycles of regeneration in comparison to the fresh sample. This behavior indicates that the amino acid anion based ionic liquids are regenerable and stable under practicable situations of regeneration. The CO_2 absorption values of IL1 are obtained 0.340, 0.340, 0.339, 0.337, 0.336, and 0.3315 in six sequential cycles of absorption/desorption and the regeneration yield IL1 is 98.8% after six consecutive cycle absorption/desorption.

Table 6
The stable absorption energies of (E_{ads}) between CO_2 and [B_4MPyr][AA]s.

[B_4MPyr][AA]	E_{ads}/ kJ•mol^{-1}
IL1	-397.33
IL2	-362.49
IL3	-360.82
IL4	-351.75
IL5	-347.86
IL6	-343.49
IL7	-315.27
IL8	-236.32

3.6. DFT calculations

3.6.1. Geometry optimization

DFT computation was applied to assess the relative affinity of the [B_4MPyr][AA]s on CO_2 absorption. At first, various structures of the modeled ionic liquids were chosen according to the partial charge dispensation and investigated. Afterwards, the most stable structures were considered to analyze the absorption of CO_2. Several mechanisms for CO_2 capture were suggested and discussed from a different molecular point of view. The optimized structures of the complexes are demonstrated in Fig. 5. To characterize the most probable structures of the cations and anions in the AAILs, B3LYP–D3/6–311++G* (d, p) calculations were carried out on the structures. The absorption energy (E_{ads}) are calculated by Eq. 9 which obtained values are listed in Table 6. The stable absorption energies of [B_4MPyr][AA]s–CO_2 follows as order: IL1 > IL2 > IL3 > IL4 > IL5 > IL6 > IL7 > IL8. This behavior is attributed to the alkyl chain length and number of amine groups as explained above. The process of CO_2 absorption in [B_4MPyr][AA]s is the result of the forming of carbamate by the absorption of CO_2 gas onto the nitrogen atom of the amino acid. The molecular path offered for the CO_2 absorption mechanism with these [B_4MPyr][AA]s has foretell the most probable site of the CO_2 absorption onto the N atom of the amino acid. According to the proposed mechanism, the reduction of C28-N1 bond length corroborates the corresponding bond–forming, while the increment of the bond distances of N1-H2 causes the bond cleavage. These geometrical alterations verify CO_2 absorption in the [B_4MPyr][AA]s.

3.6.2. Thermodynamic analysis

Thermodynamic parameters of the CO_2 absorption onto [B_4MPyr][AA]s were assessed using DFT computations. The variations of entropy, Gibbs energies, and enthalpy the CO_2 absorption on [B_4MPy][AA]s were reported in Table 7. The calculated Gibbs energies variations in CO_2 absorption reveal that IL1 is the best candidate for CO_2 absorption that is in agreement with the experimental outcomes. The parameters of thermodynamics corresponding transition state of CO_2 absorption onto [B_4MPyr][AA]s were evaluated using DFT calculations. The theoretical tendency in the reactivity of the investigated [B4MPyr][AA]s toward CO_2 absorption varied with the difference of anion as: [Arg] > [Lys] > [His] > [Tyr] > [Gly] > [Val] > [Ala] > [Pro]. This trend expresses that the anion

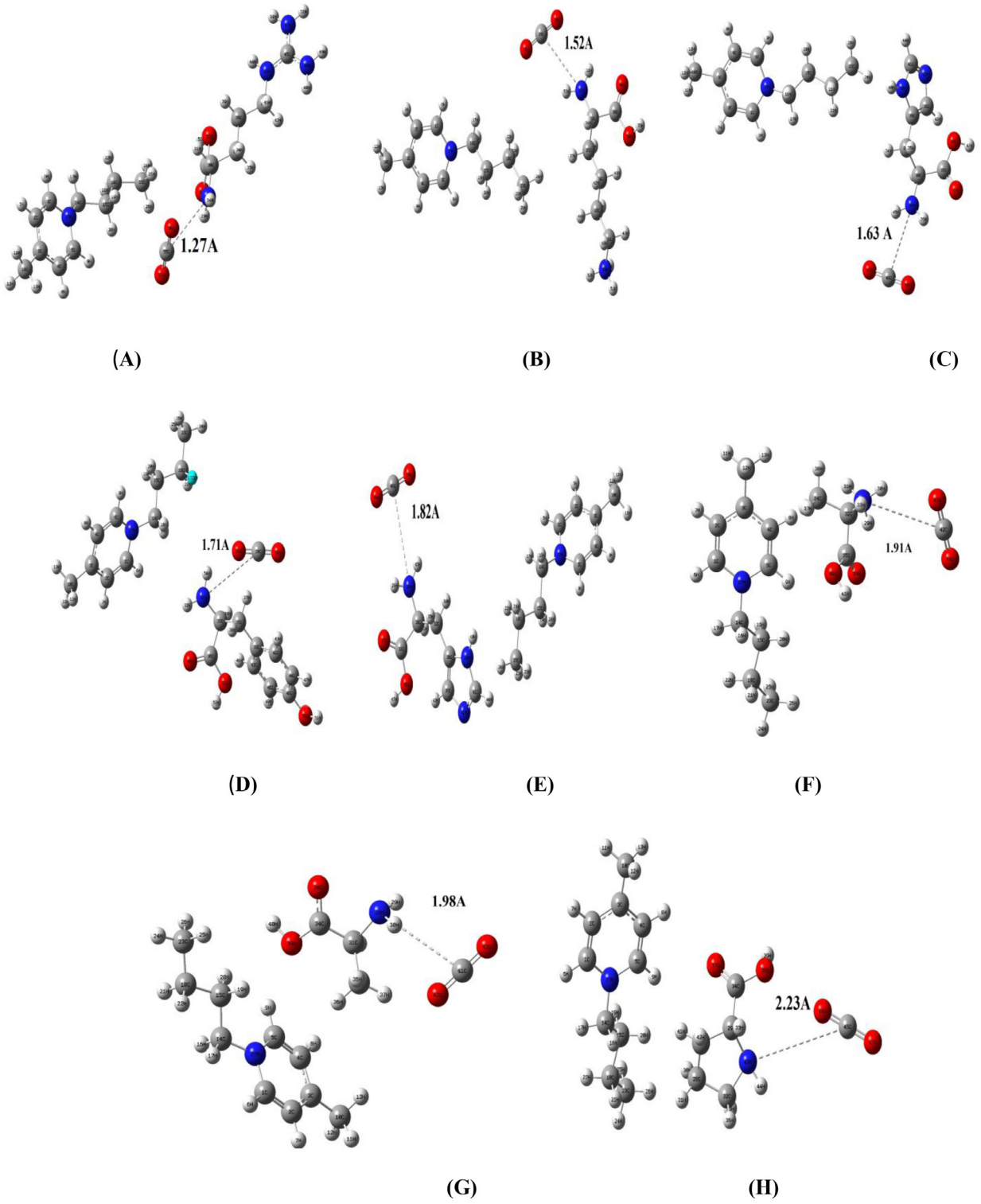

Fig. 5. Optimized structures of the complex (A) IL1−CO_2, (B) IL2–CO_2, (C) IL3−CO_2,(D) IL4−CO_2,(E) IL5−CO_2,(F) IL6−CO_2, (G) IL7−CO_2, and (H) IL8−CO_2.

has a main role in the process of CO_2 absorption. On the basis of the transition state data, an increment in the amine group of the amino acid increments the rate and extent of the reaction, which suggests IL1 is appropriate candidate for CO_2 absorption.

3.6.3. Natural bond orbital analysis

Analysis of natural bond orbital (NBO) is performed to evaluate the stabilization energy, $E^{(2)}$, by the second-order perturbation theory [64,65]. The calculated data of analysis of NBO were tabulated in Table 8. The $E^{(2)}$ value represents the intensity of the interactions among the electron donors and acceptors orbital. The donor-acceptor interactions in [B_4MPyr][AA]s are related to lone

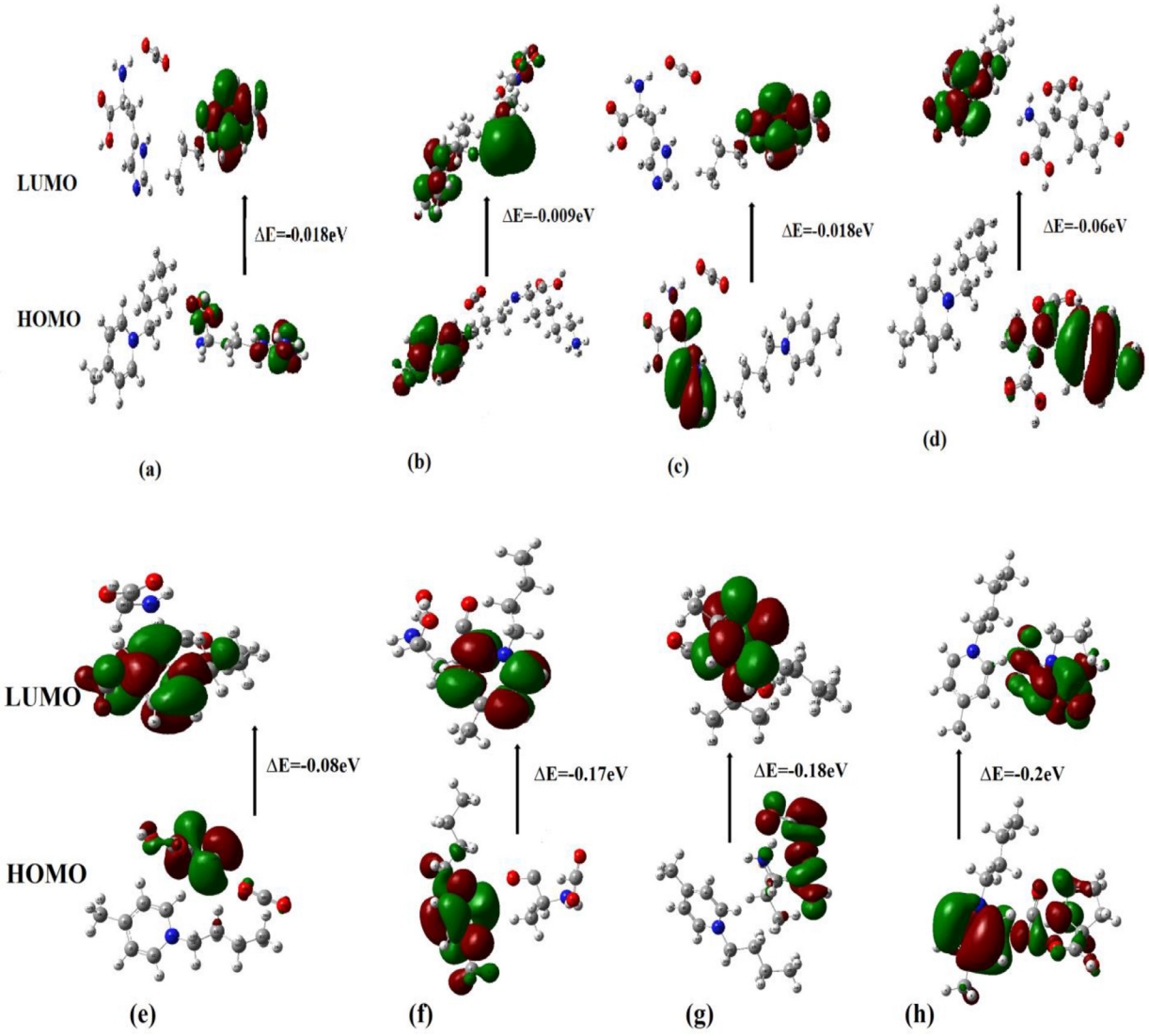

Fig. 6. The atomic orbital compositions of the frontier molecular orbital for (a) IL1−CO_2, (b) IL2−CO_2, (c) IL3−CO_2, (d) IL4−CO_2, (e) IL5−CO_2, (f) IL6−CO_2, (g) IL7−CO_2, and (h) IL8−CO_2.

Table 7
Thermodynamic and transition state parameters of the CO_2 adsorption onto [B_4MPyr][AA]s at T = 298.15 K.

	Thermodynamic parameters			Transition state parameters			
[B_4MPy][AA]	ΔG(kJ•mol^{-1})	ΔH (kJ•mol^{-1})	ΔS(J•mol^{-1}•K^{-1})	ΔG$^{\neq}$ (kJ•mol^{-1})	ΔH$^{\neq}$ (kJ•mol^{-1})	ΔS $^{\neq}$(J•mol^{-1}•K^{-1})	E_a(kJ•mol^{-1})
IL1	-50.15	-49.92	0.77	27.23	27.04	0.64	29.52
IL2	-39.82	-39.62	0.67	44.82	44.65	0.57	47.13
IL3	-38.84	-38.69	0.50	45.87	45.71	0.53	48.19
IL4	-36.19	-36.06	0.44	47.99	47.84	0.50	50.47
IL5	-28.29	-28.18	0.37	49.34	49.21	0.44	51.69
IL6	-24.87	-24.76	0.37	49.46	49.33	0.44	51.81
IL7	-20.24	-20.15	0.30	51.34	51.23	0.37	53.70
IL8	-10.28	-10.23	0.17	66.29	66.10	0.27	68.49

pair electrons of N1 interact with the anti-bonding orbital of C ($n_{N1}\rightarrow\sigma^*_{C8-O30}$) which interactions N1–C28 confirm the CO_2 absorption in the anion of amino acid.

3.6.4. Molecular orbital analysis

To investigate the mechanism of CO_2 absorption in AAILs, we interpreted the energy process based on molecular orbital. The band energetic and the localization of highest occupied molecular orbital (HOMO) and lowest unoccupied molecular orbital (LUMO) which represent the frontier molecular orbital energies of [B_4MPyr][AA]s–CO_2 are illustrated in Fig. 6. The transitions of HOMO→LUMO expose the electron density will transfer from the amine group of the anion to carbon of carbon dioxide (the HOMO is the π molecular orbital of the nitrogen and the LUMO is the π^* orbital). The decrease of the HOMO→LUMO energy gap exerts the major efficacy on the intermolecular charge transfer phenomenon due to overlapping p orbital. The lowest band gap of Argenine displays that it does not need much energy to excite the molecule and as a result causes to interact between CO_2 and Argenine; while, the

Table 8
Second order perturbation energies $E^{(2)}$ (donor → acceptor) for $[B_4MPyr][AA]-CO_2$ complexes.

$[B_4MPyr][AA]-CO_2$	Donor	Acceptor	$E^{(2)}$ (kJ•mol^{-1})
IL1−CO_2	LP (O29)	σ^* (C28–O30)	51.55
	LP (O30)	σ^* (C28–O29)	21.87
	LP (N1)	σ^* (C28–O30)	17.21
IL2−CO_2	LP (O28)	σ^* (C25–O27)	64.87
	LP (O27)	σ^* (C25–O28)	24.92
	LP (N1)	σ^* (C25–O28)	19.84
IL3−CO_2	LP (O22)	σ^* (C21–O23)	67.30
	LP (O23)	σ^* (C21–O22)	25.10
	LP (N1)	σ^* (C21–O23)	24.87
IL4−CO_2	LP (O26)	σ^* (C25–O27)	72.44
	LP (O27)	σ^* (C25–O26)	28.32
	LP (N1)	σ^* (C25–O27)	25.67
IL5−CO_2	LP (O12)	σ^* (C11–O13)	89.12
	LP (O13)	σ^* (C11–O12)	31.38
	LP (N1)	σ^* (C11–O13)	33.14
IL6−CO_2	LP (O15)	σ^* (C14–O16)	92.60
	LP (O16)	σ^* (C14–O15)	42.65
	LP (N1)	σ^* (C14–O16)	35.17
IL7−CO_2	LP (O21)	σ^* (C20–O22)	106.41
	LP (O22)	σ^* (C20–O21)	46.34
	LP (N1)	σ^* (C20–O22)	38.90
IL8−CO_2	LP (O19)	σ^* (C18–O20)	230.37
	LP (O20)	σ^* (C18–O19)	76.484
	LP (N1)	σ^* (C18–O20)	68.89

highest band gap in proline can be due to the low interaction with CO_2.

4. Conclusions

CO_2 absorption in different amino acid-based ionic liquids ($[B_4MPyr][AA]$s) has been studied at temperature 298.15 K. To assess physical and chemical absorption contributions a deactivated model has been applied. The results manifest that the CO_2 absorption in $[B_4MPyr][AA]$s is generally attributed to chemical absorption. The FT–IR spectroscopy of the CO_2 absorbed $[B_4MPyr][AA]$s indicates the formation of carbamate species. A various aminates with primary and secondary amines were considered to study the effect of the amino acid anion nature onto CO_2 absorption capacity. Among of $[B_4MPyr][AA]$s investigated, IL1 has the highest CO_2 absorption capacity and IL8 has the lowest CO_2 absorption capacity. This phenomenon reveals that the $[B_4MPyr][AA]$s with several amine sites represent higher CO_2 absorption capacity than the $[B_4MPyr][AA]$s with one primary amine group. DFT analyses show that $[B_4MPyr][AA]$s with arginate anion ([Arg]) has more CO_2 absorption capacity compared to other aminates and is utilized as a favorable CO_2 adsorbent for separation of gas in industrial usage.

Declaration of Competing Interest

None.

CRediT authorship contribution statement

Narmin Noorani: Data curation, Writing – original draft, Investigation. **Abbas Mehrdad:** Conceptualization, Writing – review & editing. **Iraj Ahadzadeh:** Methodology, Visualization.

Acknowledgment

The authors would like to thank for financial support as grant No: SAD/870-970307 from University of Tabriz.

Supplementary materials

Supplementary material associated with this article can be found, in the online version, at doi:10.1016/j.fluid.2021.113185.

References

[1] D.S. Firaha, B. Kirchner, Tuning the carbon dioxide absorption in amino acid ionic liquids, ChemSusChem 9 (2016) 1–10.
[2] Z. Lei, C. Dai, B. Chen, Gas solubility in ionic liquids, Chem. Rev. 114 (2014) 1289–1326.
[3] M. Pan, C. Wang, in: Recent Advances in CO_2 Capture by Functionalized Ionic Liquids, Advances in CO_2 Capture, Sequestration, and Conversion, American Chemical Society, Washington, DC, 2015, pp. 341–369.
[4] J.M. Matter, M. Stute, S.O. Snaebjornsdottir, E.H. Oelkers, S.R. Gislason, E.S. Aradottir, B. Sigfusson, I. Gunnarsson, H. Sigurdardottir, E. Gunnlaugsson, G. Axelsson, H.A. Alfredsson, D. Wolff-Boenisch, K. Mesfin, D.F.D.I.R. Taya, J. Hall, K. Dideriksen, W.S. Broecker, Rapid carbon mineralization for permanent disposal of anthropogenic carbon dioxide emissions, Science 352 (2016) 1312–1314.
[5] B. Li, Y. Chena, Zh. Yang, X. Ji, X. Lu, Thermodynamic study on carbon dioxide absorption in aqueous solutions of choline-based amino acid ionic liquids, Sep. Purif. Technol. 214 (2019) 128–138.
[6] D.W. Keith, Why capture CO_2 from the atmosphere? Science 325 (2009) 1654–1655.
[7] G.T. Rochelle, Amine scrubbing for CO_2 capture, Science 325 (2009) 1652–1654.
[8] T.M. McDonald, J.A. Mason, X.Q. Kong, E.D. Bloch, D. Gygi, A. Dani, V. Crocella, F. Giordanin, S.O. Odoh, W.S. Drisdell, A.L.Dzubak B.Vlaisavljevich, R. Poloni, S.K. Schnell, N. Planas, K. Lee, T. Pascal, L.W.F. Wan, D. Prendergast, J.B. Neaton, B. Smit, J.B. Kortright, L. Gagliardi, S. Bordiga, J.A. Reimer, J.R. Long, Cooperative insertion of CO_2 in diamine-appended metal-organic frameworks, Nature 519 (2015) 303–304.
[9] M.J. Li, U. Tumuluri, S.Dai Z.L.Wu, Effect of dopants on the adsorption of carbon dioxide on ceria surfaces, Chemsuschem 8 (2015) 3651–3660.
[10] K.M. Nelson, S.M. Mahurin, R.T. Mayes, B. Williamson, C.M. Teague, A.J. Binder, L. Baggetto, G.M. Veith, S. Dai, Preparation and CO_2 adsorption properties of soft-templated mesoporous carbons derived from chestnut tannin precursors, Microporous Mesoporous Mater. 222 (2016) 94–103.
[11] T. De Baerdemaeker, D. De Vos, Gas separation trapdoors in zeolites, Nat. Chem. 5 (2013) 89–90.
[12] S.M. Mahurin, J.S. Lee, H.M.Luo G.A.Baker, S. Dai, Performance of nitrile-containing anions in task-specific ionic liquids for improved CO_2/N_2 separation, J. Membr. Sci. 353 (2010) 177–183.
[13] R.T. Woodward, L.A. Stevens, R. Dawson, M. Vijayaraghavan, T. Hasell, I.P. Silverwood, A.V. Ewing, T. Ratvijitvech, J.D. Exley, S.Y. Chong, F. Blanc, D.J. Adams, S.G. Kazarian, C.E. Snape, T.C. Drage, A.I. Cooper, Swellable, water- and acid–tolerant polymer sponges for chemoselective carbon dioxide capture, J. Am. Chem. Soc. 136 (2014) 9028–9035.
[14] G.K. Cui, J.J. Wang, S.J. Zhang, Active chemisorption sites in functionalized ionic liquids for carbon capture, Chem. Soc. Rev. 45 (2016) 4307–4339.
[15] M.J. Earle, J. Esperanca, M.A. Gilea, J.N.C. Lopes, L.P.N. Rebelo, J.W. Magee, K.R. Seddon, J.A. Widegren, The distillation and volatility of ionic liquids, Nature 439 (2006) 831–834.
[16] N. MacDowell, N. Florin, A. Buchard, J. Hallett, A. Galindo, G. Jackson, C.S. Adjiman, C.K. Williams, N. Shah, P. Fennell, An overview of CO_2 capture technologies, Energy Environ. Sci. 3 (2010) 1645–1669.
[17] J.E. Bara, D.E. Camper, D.L. Gin, R.D. Noble, Room-temperature ionic liquids and composite materials: platform technologies for CO_2 capture, Acc. Chem. Res. 43 (2010) 152–159.
[18] L. Vidal, M.L. Riekkola, A. Cannals, Ionic liquid-modified materials for solid-phase extraction and separation : a review, Anal. Chim. Acta 715 (2012) 19–41.
[19] L.M.G. Sanchez, G.W. Meindersma, A.B. deHaan, Solvent properties of functionalized ionic liquids for CO_2 absorption, Chem. Eng. Res. Des. 85 (2007) 31–39.
[20] Y.S. Kim, W.Y. Choi, J.H. Jang, K.P. Yoo, C.S. Lee, Solubility measurement and prediction of carbon dioxide in ionic liquids, Fluid Phase Equilibria 228–229 (2005) 439–445.
[21] P. Sharma, S.D. Park, K.T. Park, S.C. Nam, S.K. Jeong, Y. Yoon, Y. Baek, Solubility of carbon dioxide in amine-functionalized ionic liquids: role of the anions, Chem. Eng. J. 193–194 (2012) 267–275.
[22] E.D. Bates, R.D. Mayton, I. Ntai, J.H. Davis, CO_2 capture by a task specific ionic liquid, J. Am. Chem. Soc. 124 (2002) 926–927.
[23] Y.S. Sistla, A. Khanna, CO_2 absorption studies in amine functionalized ionic liquids, J. Ind. Eng. Chem. 20 (2014) 2497–2509.
[24] K. Fukumoto, M. Yoshizawa, H. Ohno, Room temperature ionic liquids from 20 natural amino acids, J. Am. Chem. Soc. 127 (2005) 2398–2399.
[25] B.E. Gurkan, T.R. Gohndrone, M.J. McCready, J.F. Brennecke, Reaction kinetics of CO_2 absorption in to phosphonium based anion-functionalized ionic liquids, Phys. Chem. Chem. Phys. 15 (2013) 7796–7811.
[26] C.M. Wang, H.M. Luo, H.R. Li, X. Zhu, B. Yu, S. Dai, Tuning the physicochemical properties of diverse phenolic ionic liquids for equimolar CO_2 capture by the substituent on the anion, Chem. Eur. J. 18 (2012) 2153–2160.
[27] B.E. Gurkan, J.C. de la Fuente, E.M. Mindrup, L.E. Ficke, B.F. Goodrich, E.A. Price, W.F. Schneider, J.F. Brennecke, Equimolar CO_2 absorption by anion-functionalized ionic liquids, J. Am. Chem. Soc. 132 (2010) 2116–2117.

[28] F.F. Chen, K. Huang, Y. Zhou, Z.Q. Tian, X. Zhu, D.J. Tao, D. Jiang, S. Dai, Multimolar absorption of CO_2 by the activation of carboxylate groups in amino acid ionic liquids, Angew. Chem. Int. Ed. 55 (2016) 7166–7170.
[29] H.J. Song, S. Park, H. Kim, A. Gaur, J.W. Park, S.J. Lee, Carbon dioxide absorption characteristics of aqueous amino acid salt solutions, Int. J. Greenh. Gas Control 11 (2012) 64–72.
[30] J.W. Ma, Z. Zhou, F. Zhang, G.G. Fang, Y.T. Wu, Z.B. Zhang, A.M. Li, Ditetraalkylammonium amino acid ionic liquids as CO_2 absorbents of high capacity, Environ. Sci. Technol. 45 (2011) 10627–10633.
[31] S.h. Saravanamurugan, A.J.F.R. Kunov-Kruse, A. Riisager, Amine-Functionalized Amino Acid-based Ionic Liquids as Efficient and High-Capacity Absorbents for CO_2, ChemSusChem 7 (2014) 897–902.
[32] Z. Zhou, X. Zhou, G. Jing, B. Lv, Evaluation of multi-amine functionalized ionic liquid for efficient post-combustion CO_2 capture, Energy Fuels 30 (2016) 7489–7495.
[33] Y. Zhang, S. Zhang, X. Lu, Q. Zhou, W. Fan, W.P. Zhang, Dual aminofunctionalised phosphonium ionic liquids for CO_2 capture, Chem. Eur. J. 15 (2009) 3003–3011.
[34] N. Noorani, A. Mehrdad, CO_2 solubility in some amino acid-based ionic liquids: measurement,correlation and DFT studies, Fluid Phase Equilibria 517 (2020) 112591.
[35] N. Noorani, A. Mehrdad, Experimental and theoretical study of CO_2 sorption in biocompatible and biodegradable cholinium-based ionic liquids, Sep. Purif. Technol. 254 (2021) 117609.
[36] A. Mehrdad, H. Shekaari, N. Noorani, Density, speed of sound, and viscosity of aqueous solutions containing 1-alkyl-4-methylpyridinium bromide, lactic acid, and polyethylene glycol, J. Chem. Eng. Data 62 (2017) 2021–2029.
[37] A. Mehrdad, H. Shekaari, N. Noorani, Effect of 1–butyl–4–methylpyridinium and 1–butyl–3–methylimidazolium halide ionic liquids on the interactions of lactic acid in the aqueous solutions of polyethylene glycol, J. Chem.Thermodyn. 112 (2017) 188–195.
[38] A. Stark, D. Ott, D. Kralisch, G. Kreisel, B. Ondruschka, Ionic liquids and green chemistry: a lab experiment, J. Chem. Educ. 87 (2010) 196–201.
[39] N. Noorani, A. Mehrdad, F. Chakhmaghi, Thermodynamic study on carbon dioxide and methane permeability in polyvinylchloride/ionic liquid blends, J. Chem. Thermodyn. 145 (2020) 106094.
[40] A. Mehrdad, N. Noorani, Study of CO_2 adsorption onto poly(1–vinylimidazole) using quartz crystal microbalance and density functional theory methods, J. Mol. Liq. 291 (2019) 111288.
[41] N. Noorani, A. Mehrdad, Adsorption, permeation, and DFT studies of PVC/PVIm blends for separation of CO_2/CH_4, J. Mol. Liq. 292 (2019) 111410.
[42] N. Noorani, A. Mehrdad, Modification of PVC with 1-vinylimidazole for CO_2/CH_4 separation: sorption, permeation and DFT studies, Phys. Chem. Res. 8 (2020) 689–703.
[43] C. Moya, N. Alonso-Morales, J. Riva, O. Morales-Collazo, J.F. Brennecke, J. Palomar, Encapsulation of ionic liquids with an aprotic heterocyclic anion (AHAIL) for CO_2 capture: preserving the favorable thermodynamics and enhancing the kinetics of absorption, J. Phys. Chem. B 122 (2018) 2616–2626.
[44] Xiong W, M. Shi a, L. Peng, X. Zhang, X. Hu, Y.T. Wu, Low viscosity superbase protic ionic liquids for the highly efficient simultaneous removal of H2S and CO2 from CH4, Sep. Purif. Technol. 263 (2021) 118417.
[45] X.M. Zhang, K. Huang, Sh. Xia, Y.L. Chen, Y.T. Wu, X.B. Hu, Low-viscous fluorine-substituted phenolic ionic liquids with high performance for capture of CO2, Chem. Eng. J. 274 (2015) 30–38.
[46] M.J. Frisch, G.W. Trucks, H.B. Schlegel, G.E. Scuseria, M.A. Robb, J.R. Cheeseman, J.A. Montgomery, T. Vreven, K.N. Kudin, J.C. Burant, J.M. Millam, S.S. Iyengar, J. Tomasi, V. Barone, B. Mennucci, M. Cossi, G. Scalmani, N. Rega, G.A. Petersson, H. Nakatsuji, M. Hada, M. Ehara, K. Toyota, R. Fukuda, J. Hasegawa, M. Ishida, T. Nakajima, Y. Honda, O. Kitao, H. Nakai, M. Klene, X. Li, J.E. Knox, H.P. Hratchian, J.B. Cross, V. Bakken, C. Adamo, J. Jaramillo, R. Gomperts, R.E. Stratmann, O. Yazyev, A.J. Austin, R. Cammi, C. Pomelli, J.W. Ochterski, P.Y. Ayala, K. Morokuma, G.A. Voth, P. Salvador, J.J. Dannenberg, V.G. Zakrzewski, S. Dapprich, A.D. Daniels, M.C. Strain, O. Farkas, D.K. Malick, A.D. Rabuck, K. Raghavachari, J.B. Foresman, J.V. Ortiz, Q. Cui, A.G. Baboul, S. Clifford, J. Cioslowski, B.B. Stefanov, G. Liu, A. Liashenko, P. Piskorz, I. Komaromi, R.L. Martin, D.J. Fox, T. Keith, A. Laham, C.Y. Peng, A. Nanayakkara, M. Challacombe, P.M.W. Gill, B. Johnson, W. Chen, M.W. Wong, C. Gonzalez, J.A. Pople, Gaussian 03. Revision B.03., Gaussian, Inc., Pittsburgh, 2003.
[47] A.D. Becke, Density-functional thermochemistry. III. The role of exact exchange, J. Chem. Phys. 98 (1993) 5648–5652.
[48] C. Lee, W. Yang, R.G. Parr, Development of the Colle–Salvetti correlation-energy formula into a functional of the electron density, Phys. Rev. B 37 (1988) 785–789.
[49] A. Mehrdad, N. Noorani, Permeability behavior of polyvinyl chloride-ionic liquid ionomer for CO_2/CH_4 separation, Sep. Purif. Technol. 226 (2019) 138–145.
[50] X. Zhang, W. Xiong, L. Peng, Y. Wu, X. Hu, Highly selective absorption separation of H_2S and CO_2 from CH_4 by novel azole-based protic ionic liquids, AIChE J. 66 (2020) 16936.
[51] X. Zhang, W. Xiong, Zh. Tu, L. Peng, Y. Wu, X. Hu, Supported ionic liquid membranes with dual-site interaction mechanism for efficient separation of CO_2, ACS Sustain. Chem. Eng. 7 (2019) 10792–10799.
[52] E.D. Glendening, A.E. Reed, J.E. Carpenter, F. Weinhold, NBO 3.0 Program Manual, Gaussian Inc, Pittsburgh, 1995.
[53] A. Barth, The infrared absorption of amino acid side chains, Prog. Biophys. Mol. Biol. 74 (2000) 141–173.
[54] X. Zhang, W. Xiong, M. Shi, Y. Wu, Xi Hu, Task-specific ionic liquids as absorbents and catalysts for efficient capture and conversion of H2S into value-added mercaptan acids, Chem. Eng. J. 408 (2021) 127866.
[55] K. Huang, Y.L. Chen, X.M. Zhang, S. Xia, Y.T. Wu, X.B. Hu, SO_2 absorption in acid salt ionic liquids/sulfolane binary mixtures: Experimental study and thermodynamic analysis, Chem. Eng. J. 237 (2014) 478–486.
[56] X.S. Li, L.Q. Zhang, Y. Zheng, C.G. Zheng, Effect of SO_2 on CO_2 absorption in flue gas by ionic liquid 1-ethyl-3-methylimidazolium acetate, Ind. Eng. Chem. Res. 54 (2015) 8569–8578.
[57] M. Ramdin, T.W. de Loos, T.J. Vlugt, State-of-the-art of CO_2 capture with ionic liquids, Ind. Eng. Chem. Res. 51 (2012) 8149–8177.
[58] B.F. Goodrich, J.C. de la Fuente, B.E. Gurkan, D.J. Zadigian, E.A. Price, Y. Huang, J.F. Brennecke, Experimental measurements of amine-functionalized anion-tethered ionic liquids with carbon dioxide, Ind. Eng. Chem. Res. 50 (2011) 111–118.
[59] M. Aghaie, N. Rezaei, S. Zendehboudi, A systematic review on CO_2 capture with ionic liquids: current status and future prospects, Renew. Sustain. Energy Rev. 96 (2018) 502–525.
[60] J. McMurry, in: Fundamentals of Organic Chemistry, 7th Ed., Cengage Learning, USA, 2011, pp. 506–507.
[61] R. Santiago, J. Lemus, Ch. Moya, D. Moreno, N. Alonso-Morales, J. Palomar, Encapsulated ionic liquids to enable the practical application of amino acid-based ionic liquids in CO_2 capture, ACS Sustain. Chem. Eng. 6 (2018) 14178–14187.
[62] M. Sh. Raja Shahrom, C.D. Wilfred, D.R. MacFarlane, R. Vijayraghavan, Ch.F. Kait, Amino acid based poly(ionic liquid) materials for CO_2 capture: effect of anion, J. Mol. Liq. 25 (2019) 644–652.
[63] M.Sh.Raja Shahrom, C.D. Wilfred, A. Khidir Ziyada Taha, CO_2 capture by task specific ionic liquids (TSILs) and polymerized ionic liquids (PILs and AAPILs), J. Mol. Liq. 219 (2016) 306–312.
[64] S. Subash chandrabose, A.R. Krishnana, H. Saleem, R. Paramashwari, N. Sundaraganesan, V. Thanikachalam, G. Maikandan, Vibrational spectroscopic study and NBO analysis on bis(4-amino-5-mercapto-1,2,4-triazol-3-yl) methane using DFT method, Spectrochim. Acta. 77A (2010) 877–884.
[65] C. James, A. Amal raj, R. Reghunathan, I.H. Joe, V.S. Jayakumar, Structural conformation and vibrational spectroscopic studies of 2,6-bis(*p*-*N*,*N*-dimethyl benzylidene)cyclohexanone using density functional theory, J. Raman Spectrosoc. 37 (2006) 1381–1392.